Understanding the helical stability of charged peptides

Nitin Kumar Singh[1], Manish Agarwal[2], and Mithun Radhakrishna[1]

[1]Indian Institute of Technology Gandhinagar
[2]Indian Institute of Technology Delhi

July 6, 2022

Abstract

Cationic helical peptides play a crucial role in applications such as anti-microbial and anti-cancer activity. The activity of these peptides directly correlates with their helicity. In this study, we have performed extensive all-atom molecular dynamics simulations of 25 Lysine-Leucine co-polypeptide sequences of varying charge density (λ) and patterns. Our findings showed that an increase in the charge density on the peptide leads to a gradual decrease in the helicity up to a critical charge density λ_c . Beyond, λ_c a complete helix to coil transition was observed. The decrease in the helicity correlated with the increased number of water molecules in first solvation shell, solvent-exposed surface area, and a higher value of the radius of gyration of the peptide.

Understanding the helical stability of charged peptides

Nitin Kumar Singh,[†] Manish Agarwal,[‡] and Mithun Radhakrishna[*,†,¶]

†*Discipline of Chemical Engineering, Indian Institute of Technology (IIT) Gandhinagar, Palaj, Gujarat 382355, India*

‡*Computer Services Centre, Indian Institute of Technology (IIT) Delhi, Hauz Khas, New Delhi, Delhi 110016*

¶*Center for Biomedical Engineering, Indian Institute of Technology (IIT) Gandhinagar, Palaj, Gujarat 382355, India*

E-mail: mithunr@iitgn.ac.in,zmanish@cc.iitd.ac.in

Abstract

Cationic helical peptides play a crucial role in applications such as anti-microbial and anti-cancer activity. The activity of these peptides directly correlates with their helicity. In this study, we have performed extensive all-atom molecular dynamics simulations of 25 Lysine-Leucine co-polypeptide sequences of varying charge density (λ) and patterns. Our findings showed that an increase in the charge density on the peptide leads to a gradual decrease in the helicity up to a critical charge density λ_c. Beyond, λ_c a complete helix to coil transition was observed. The decrease in the helicity correlated with the increased number of water molecules in first solvation shell, solvent-exposed surface area, and a higher value of the radius of gyration of the peptide.

Introduction

The spontaneous folding of the proteins into the secondary structure plays a crucial role in the biological functioning of the protein. Folding into secondary structures is driven by inter molecular interactions such as hydrogen bonding, electrostatics, hydrophobic effect and the van der waals interaction between the amino acids of peptide chain. The secondary structures are generally classified into classes such as, α-helix, G_{10}-helix, π-helix, β-sheets, turns and coils based on backbone dihedral angles. Among these, the α-helices and β-sheets are the most prevalent secondary structures.[1] α-helices are motifs with exceptional folding/unfolding property and a rigid rod-framework, and they have been largely used as a building block in the design of molecular assemblies and small amphiphilic peptides.[2–4] These are the most regular form in the secondary structure of protein, and play a cooperative role in protein folding.[5,6] Some of the well known proteins such as Hemoglobin, Myoglobin, Keratin, Human cytochrome c oxidase, GINS protein complex, RNA polymerases, Human respiratory complex, etc possess a very high helical content.[7] The α-helix structure has shown its application in the various domains, such as membrane interactions, anti-microbial activity[8–11] and anti-cancer activity.[12–14]Helical motifs have also been used as binding domains to high value targets such as BCL2 and HIV protein gp41.[15,16] Along with these, they also have role in mediating protein interaction with other biomolecules such as DNA and RNA.

Because of the vast applications and their abundance in the protein structure, α-helices have been studied extensively using both experimental and computational tools.[17–19] Most of the previous studies have focused on understanding the stability of short helical peptides of poly-L-alanine, poly-L-glutamic acid, poly-L-lysine. Berger et. al. studied the helical stability of poly-DL-Alanine using the deuterium exchange method and observed that the exchange rate was catalysed by both hydrogen and hydroxyl ions.[20] Ferrati et. al. have captured the helix-coil transition of alanine peptide that occurrs at short time interval using nuclear magnetic resonance(NMR).[21] Levitt et. al. performed computer simulations of 13 residue peptide to study the helical behaviour in vacuum and solvent, and they observed an

unfolding of the peptide in solvent medium.[22] Bixon et. al. studied the solvent effect for the stability of the helical structures.[23] Their finding showed that the helical structure was dictated by a fine balance between peptide-water and intra-peptide hydrogen bonding.

Previous studies have focused on the the design of α-helices comprising of hydrophobic residues or sequence of positive and negative residues.[24] In one of the very first study addressing the helical stability, Doty et. al. studied the stability of the poly-L-Glutamic acid and reported that the helix to coil transition was observed when the peptide sequence contained at least 40% of the charged residues.[25] Nishigami et. al. studied the helical stability of co-polypeptide comprising of Lysine and Glutamic acid. They observed that the maximum helical propensity was found at the boundary of Lysine and Glutamic acid.[26] Further, many studies have focused on the patterning of charged residues and have shown that distance and ordering of positive and negative residues in the sequence plays an important role on the helical stability. These studies have attributed this to the change in the salt bridge forming propensity of the amino acids.[27–29] Furthermore, the presence of the charged residues also affects the transport properties and solubility due to the presence of dipole moment and net charge in protein.

α-helical anti-cancer peptides (α-ACPs) have a large proportion of positively charged residues like Lysine and Arginine in abundance, resulting in a net positive charge on helix. The interaction of the α-helical anti-cancer peptides (α-ACPs) with the tumor cell membrane causes apoptosis and it's application in the treatment of cancer is well established. The activity of α-ACPs is highly dependent on the helicity, and studies have shown that lower helicity of cationic anti-cancer peptides is associated with lowering HeLa activity.[30–32]

Many previous studies have shown that the formation of the hydrophobic packing plays a crucial role in folding of globular proteins[33–35] and residues such as Methionine, Alanine, Leucine, Lysine (uncharged) and Glutamic acid (uncharged) are known to stabilize helix. The helical stability can be controlled by changing pH, ionic strength, temperature, solvent etc. Although helices are known to contain charged residues, stabilizing the helix when the

net charge is either positive or negative is very difficult due to the electrostatic repulsion between the like charge groups of amino acid side chain.[36–40]

In the current study, we have used all-atom Molecular Dynamics simulations to understand the helical stability of 25 de-novo designed co-polypeptide sequences of Lysine and Leucine that contain net positive charges. Our study tries to address three broad questions (a) Can the helix forming ability of hydrophobic residues be leveraged to design peptide sequences containing like charged residues that fold into a helix? (b) If there exists a critical charge density that dictates the helix coil transition? (c) Does patterning of the hydrophobic and charged residues play a role in helical stability? Our findings show that the peptides containing like charges could be stabilized up to a critical charge density (λ_c) beyond which a helix to coil transition was observed. Further, our findings show that at a fixed charge density(λ), the helical stability of peptide was found to be independent of the patterning of the sequence. We believe our study could also shed some light on the behaviour of Intrinsically Disordered proteins (IDPs) and serve as a model system for studying amyloid forming small peptides.

Model and Methods

All initial configuration of homo-polypeptides (poly-leucine, poly-lysine, poly-aspartic acid, poly-glutamic acid and poly-arginine) were constructed using the Chimera software.[41] Initial configuration of all peptides were designed to be completely α-helical. The co-polypeptides containing leucine and lysine of varying charge density and patterning were also constructed as above. Charge density(λ) is defined as $\lambda = \dfrac{\sum_1^N z_i}{N}$, where z_i is the net charge on the i$^{\text{th}}$ amino acid residue and N is the total number of amino-acids in the peptide chain. For example $\lambda=0$ for homopolypeptide of Leucine (L$_{20}$) and $\lambda=1$ for Lysine (K$_{20}$). The peptides were solvated in a box of 75x75x75Å^3 with TIP3P water model and the system was neutralized by adding counter ions using solvate and autoionize plugin of VMD respectively[42] respectively.

The forcefield parameters for the peptides were derived from CHARMM36[43] force field and the simulations were carried out using NAMD (version2.13-gpu)[44] simulation engine. The solvated system was minimized for 2500 steps by means of conjugate gradient method. Multiple independent simulations were performed for each of the studied sequence for 1μs in Isothermal isobaric (NPT) ensemble with a time step of 2fs. The pressure was maintained at 1 bar using Langevin barostat method with decay period of 50ps and damping time of 100ps and temperature at 300K was controlled using Langevin dynamics.[45] The bonds involving hydrogen atoms were constrained using the SHAKE algorithm.[46] Non-bonded interactions were calculated with a cut-off value of 12Å with a switching distance of 10Å and pairlistdist was set to 14Å. The long-range electrostatic interactions were calculated using the particle-mesh Ewald summation (PME)[47] method with PMEGridSpacing of 1Å. Multiple timestep parameters were applied for the electrostatics and short-range non-bonded interaction evaluation. The number of timesteps between full electrostatics evaluation was set to 2 i.e. the PME calculations were done every other step and the nonbondedFreq was set to 1 to calculate the non-bonded forces every step. Scaled1-4 parameter is applied to exclude pairs of bonded atoms from non-bonded interactions and 1-4scaling is applied for the electrostatic interaction, required for scaled1-4 parameter. For each of the sequences studied four to eight set of independent runs for 1μs were carried out. All the thermodynamics averages were calculated using the last 200ns of the 1μs long simulation runs. Data is averaged over all independent runs. The analysis for the simulations were done using in-house Tcl and Python scripts.

Calculation of fraction of helical content (α)

The secondary structure timeline of the peptides studied is analysed using the STRIDE algorithm,[48] which is available as a plugin in VMD. The STRIDE algorithm takes into account the dihedral angles of the peptide backbone along with the hydrogen bonding distance to assign a secondary structure state to individual amino acid residue of the peptide. The frac-

tion of helical content (α) is calculated by formula $\alpha = \dfrac{n_{Helix}}{N}$, where n_{Helix} is the number of amino acids residues in the helical conformation and N is the total number of amino acids in the peptide chain.

Results and discussion

Simulations of homopolypeptides

In this study we have considered 20 residue long homo-polypeptide of Lysine (K_{20}), Arginine (R_{20}), Aspartic acid (D_{20}), Glutamic acid (E_{20}), and Leucine (L_{20}). Since the main objective of the work was to understand the effect of charge density (λ) on the helical stability, the simulations of these homopolypeptide sequences serve as control set. These set of simulations provide us information at extreme values of λ ie. $\lambda = 0$ for Leu_{20} and $\lambda = 1$ for Lys_{20}, Asp_{20}, Arg_{20} and Glu_{20}

Molecular Dynamics simulations were performed in NPT ensemble at 300K in explicit solvent. Initial set of all peptides were designed to be in α-helix. Figure 1 shows the average helical content of the homopolypeptides as a function of time. The data for the helicity is averaged over an interval of 5ns. It is evident from Figure 1 that while L_{20} retained its helicity during course of simulation, all the charged homopolypeptides unfolded and lost their helicity. This can be attributed to the electrostatic repulsion between the like charged groups of the amino acid side chains leading to the loss of intra-peptide hydrogen bonds. The electrostatic energy of the charged homopolypeptides is plotted as a function of time in Supplementary Figure S1 . In case of all the four charged peptides we see a decrease in electrostatic energy during the course of simulation, which also correlates to the unfolding of the helical polypeptide. This decrease in the energy is due to the reduced repulsion between the like charged groups of the polypeptide side chains. Table 1 shows the difference in electrostatic energy of the charged peptides in helical and unfolded state. Further, we also quantified the water-peptide and intra-peptide hydrogen bonds shown in Supplementary

Figure S2. It is very evident that for all the charged polypeptides the loss of helical content results in the loss of intra-peptide hydrogen bonds in favour of water-peptide hydrogen bonds due to the larger surface area exposed. The pair correlation function between the like charge side chains calculated for the equilibrium runs were compared with the initial α-helical state of the peptide. We see the first peak is shifted to larger distance upon unfolding for all cases indicative of increased distance between side chains resulting in reduced repulsion (Figure S3 in supplementary information).
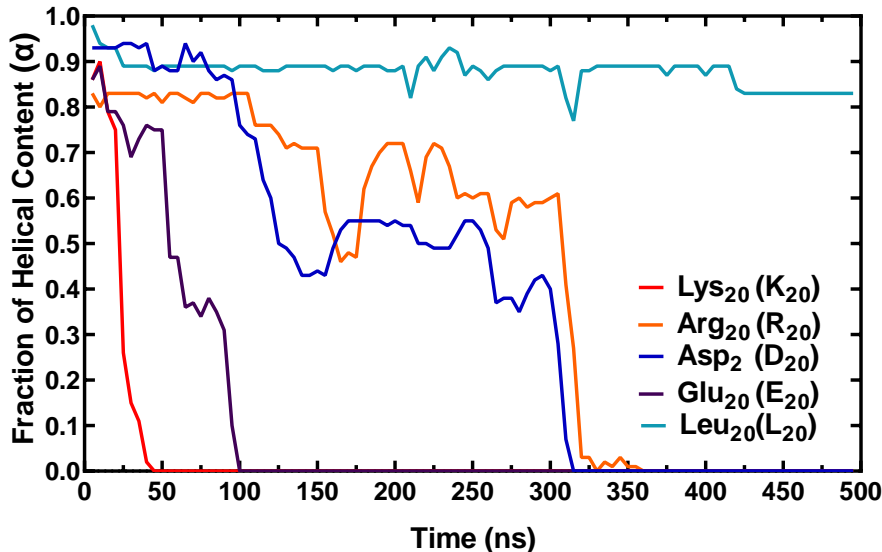

Figure 1: Fraction of helical content of homopolypeptides (K_{20}), (R_{20}), (D_{20}), (E_{20}) and (L_{20}) as function of time of simulations carried out in NPT ensemble at 300K and 1 bar

Table 1: Difference in electrostatic energies of helical and unfolded state different charged homopolypeptides.

S. No.	Peptide	$\Delta E = E_{folded} - E_{unfolded}$ (Kcal/mol)
1	K_{20}	210.47 ± 87.43
2	R_{20}	163.57 ± 86.90
3	D_{20}	443.07 ± 72.48
4	E_{20}	156.84 ± 74.69

In order to understand the effect of temperature on charged peptides, $(K)_{20}$ was chosen as a model peptide due to the application of cationic peptides in various biological functions.

Molecular Dynamics simulations of K_{20} were performed upto temperatures of 260K (it is to be noted that the melting point of the TIP3 water model is 145.6K). Figure S4 in the supplementary information shows the fraction of residues in α-helix for the K_{20} peptide at different temperatures, starting from 300K to 260K. Lowering temperature did not change the behaviour of K_{20} and the peptide unfolded at all the temperatures.

Simulations of Patterned peptides

From Figure 1, it is evident that charged homopolypeptides lose helicity and hydrophobic polypeptides retain their helicity. However, hydrophobic polypeptides are insoluble in water while charged peptides are soluble. This motivated us to explore various co-polypeptides of Lysine (K) and Leucine (L), and study the effect of charge density(λ) and patterning on the helical stability of peptides. In the current study we have designed 25 de-novo co-polypeptide sequences of λ ranging from 0.16 to 0.83. For this study, we have considered peptides containing 24 amino acid residues. Few sequences considered were of length 21,25,27 and 28 to accommodate the patterning. We know that while poly-leucine (L_{20}) is stable in the helical form, poly-lysine (K_{20}) unfolds into a coil. The sequences studied were based on the repeat units $(K_x L_y)_n$ where n is the number of repeat units and x y are integers. While most of the repeat patterns could be accommodated with N(length of the peptide) =24 for example, x=1,y=1,n=12. Few sequences, for example ($K_1 L_4$) or ($K_4 L_1$) at $\lambda = 0.2$ and 0.8 respectively, had to have residues N=25 to complete the pattern. While we understand that this is not an exhaustive list of all possible combinations of K and L co-polypeptides, it covers the entire range of λ from low to high. Figure 2 shows the pictorial representation of initial α-helical structure of various sequences studied and Table 2 provides the list of the sequences, their corresponding charge content and their length. Four to eight set of independent simulations up to $1\mu s$ were carried out for each of these sequences and the averages and error bars were calculated based on last 200 ns for each independent run.

Figure 3 shows the averaged fractional helical content (α) and the radius of gyration of

8

Table 2: 25 co-polypeptide sequences of $(K_xL_y)_n$ made of Lysine(K)-Leucine(L) and their corresponding charge content and length

| S. No.	x	y	n	N	Sequence	λ
1	1	5	4	24	$(K_1L_5)_4$	0.16
2	1	4	5	25	$(K_1L_4)_5$	0.20
3	1	3	6	24	$(K_1L_3)_6$	0.25
4	2	6	3	24	$(K_2L_6)_3$	0.25
5	3	9	2	24	$(K_3L_9)_2$	0.25
6	2	5	3	21	$(K_2L_5)_3$	0.28
7	1	2	8	24	$(K_1L_2)_8$	0.33
8	2	4	4	24	$(K_2L_4)_4$	0.33
9	3	6	3	27	$(K_3L_6)_3$	0.33
10	3	5	4	24	$(K_3L_5)_4$	0.37
11	2	3	5	25	$(K_2L_3)_5$	0.40
12	3	4	4	28	$(K_3L_4)_3$	0.42
13	4	5	3	27	$(K_4L_5)_3$	0.44
14	1	1	12	24	$(K_1L_1)_{12}$	0.50
15	2	2	6	24	$(K_2L_2)_6$	0.50
16	3	3	4	24	$(K_3L_3)_4$	0.50
17	4	4	3	24	$(K_4L_4)_3$	0.50
18	6	6	2	24	$(K_6L_6)_2$	0.50
19	4	3	4	28	$(K_4L_3)_4$	0.57
20	3	2	5	25	$(K_3L_2)_5$	0.60
21	2	1	8	24	$(K_2L_1)_8$	0.66
22	4	2	4	24	$(K_4L_2)_4$	0.66
23	3	1	6	24	$(K_3L_1)_6$	0.75
24	4	1	5	25	$(K_4L_1)_5$	0.80
25	5	1	4	24	$(K_5L_1)_4$	0.83
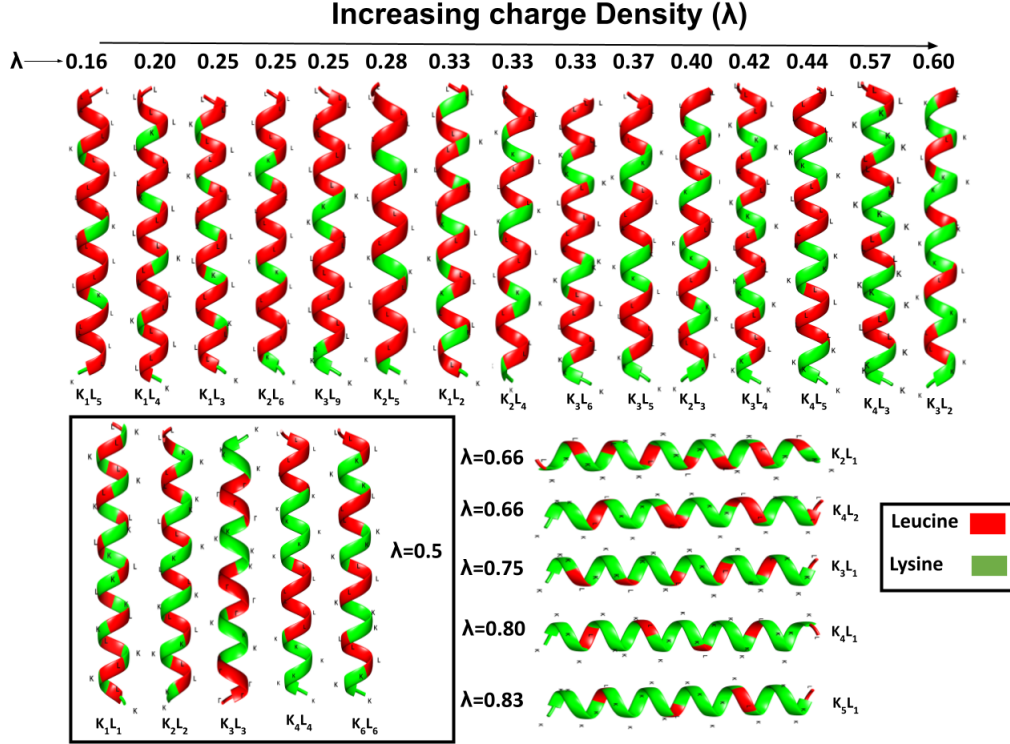
Figure 2: Pictorial representation of the initial structure of different co polypeptide sequences of Lysine and Leucine

all the 25 sequences studied. As we move from left to right there is an increase in λ with $(K_1L_5)_4$ being at 0.16 to $(K_5L_1)_4$ being at 0.83. At the outset it is clear that as λ is increased, on average there is a decrease in helical content and an increase in the radius of gyration of peptide. Further, we also observe that for $\lambda \geq 0.67$ the helical content drops to zero. Based on the trends observed, the graph can be divided into two regions. The basis for classification for these regions could be explained as follows. In region 1 ($\lambda \leq 0.60$), even though there is a gradual decrease in helicity with increasing λ, a fraction of residues still remain in the α-helical state. This is also validated by the fact that there is no dramatic change in radius of gyration of peptides. In Region 2, which comprises of sequences at high charge densities ($\lambda \geq 0.66$), we do not observe any α-helical content in the peptide with all the α-helical residues being transformed into coils. Further, the radius of gyration of peptides in region 2 is much higher than for the peptides in region 1 indicative of unfolding of α-helices. The interface between these two regions is the transition region where it is difficult to characterize

the behaviour of peptide due to the large fluctuations in the α-helical content. More precisely, the average helical content obtained from each of independent runs did not converge with few runs displaying some helicity while others displaying no helicity. Furthermore, we also observed refolding of few residues in the coil state back to helix, making the characterization difficult. This behavior is reminiscent of IDPs which change their structure dynamically and previous studies have indicated such behavior among peptide having high charge content albeit for for very specific sequences.[24,49] It is important to note that both the K and L residues contributed in almost in equal proportions towards the final helical content of the peptide.
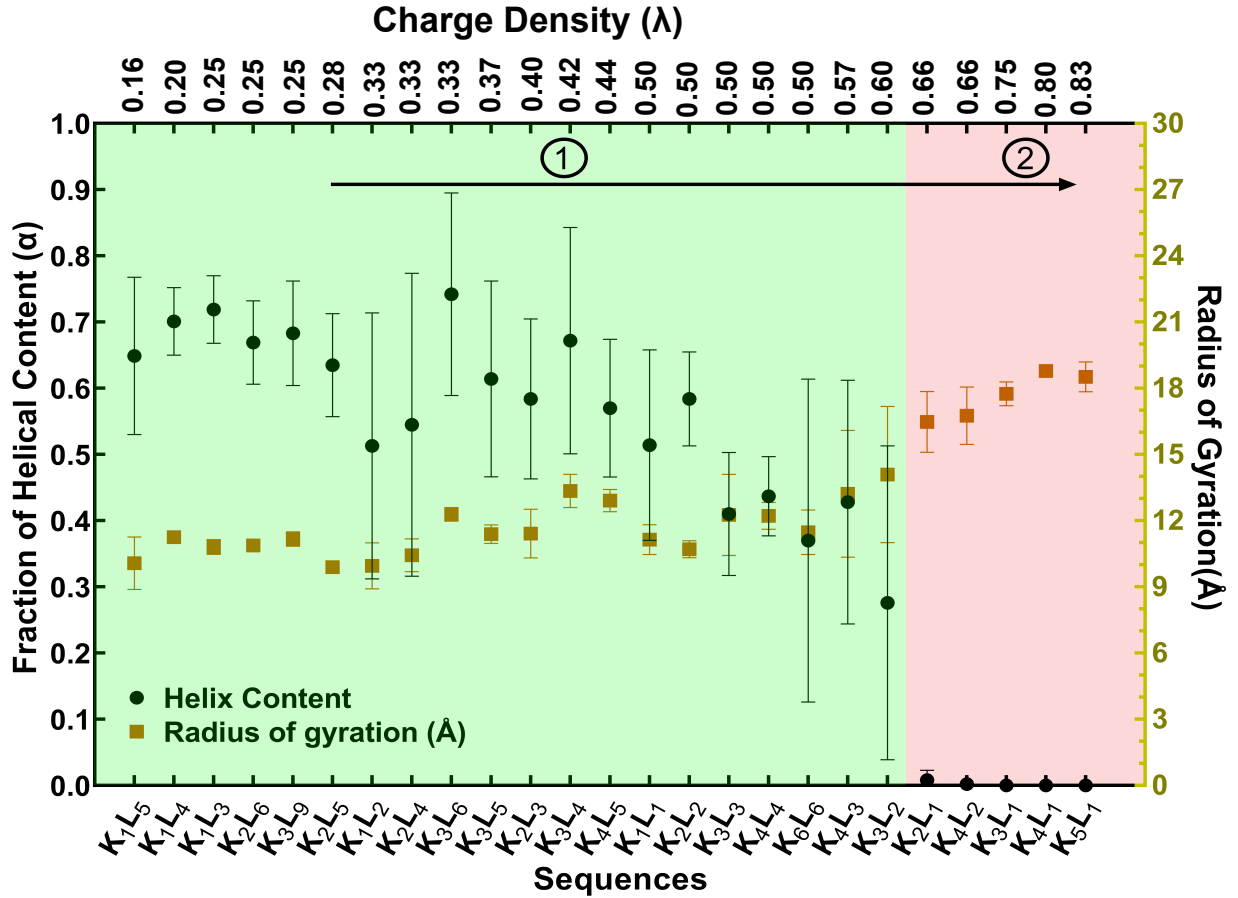

Figure 3: Fraction of α-helical content for different sequences. The fraction of the helical content decreased on increasing the charge density on the peptides

Figure 4 shows the average helical content of different peptide sequences at a fixed charge density. As the charge density is increased we see a decrease in helical content. However, at a fix charge content, we did not observe any appreciable change in the helical content for different patterns of sequences.
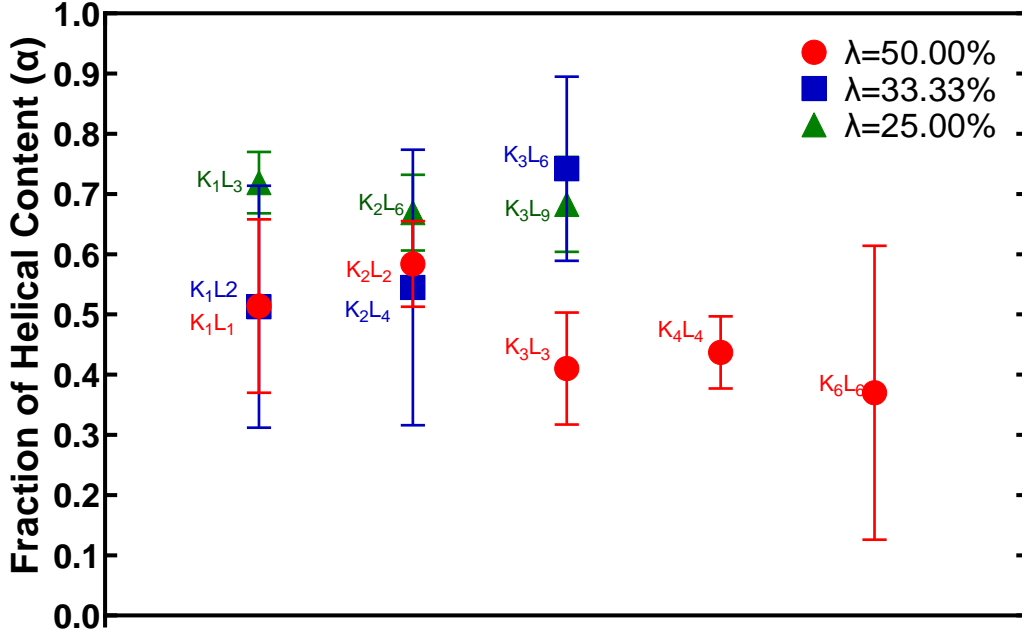

Figure 4: Fraction of helical content at fixed charge density λ of 50%, 33% and 25%

In order to quantify the above findings, we calculated the number of water molecules in the first solvation shell, the solvent accessible surface area (SASA), intra-peptide hydrogen bonds and peptide water hydrogen bonds as shown in Figure 5(a and b). For calculating the number of water molecules within the solvation shell we considered all the water molecules that lie within a radius of 6Å from the center of mass of the peptide chain. SASA was calculated using inbuilt plugin in VMD with a probe radius of 1.4Å. The averaged Radius of gyration is calculated as $\langle Rg \rangle = \left\langle \sqrt{\frac{1}{N} \sum_{1}^{N} (r_i - r_{cm})^2} \right\rangle$, where r_i is the position of center of mass of ith residue, r_{cm} is the center of mass of entire protein, N is the total number of residues and $\langle \rangle$ represents the ensemble average. With an increase in the λ, we observed a direct correlation between number of waters and the SASA. The peptide in its completely

helical state has the least SASA and consequently very small number of water molecules are present in the first solvation shell. As the value of λ of the sequence is increased, the loss in the helical content translated to an increase in the coil content of the peptide leading to enhanced SASA and increased numbers of waters in first solvation shell. Figure 5(b) shows that the peptide loses its hydrogen bonds as the charge density increases in favour of water-peptide hydrogen bonds. Figure 6 shows the electrostatic energy and van der Waal (vdW) energy for all the 25 peptide sequences studied. The electrostatic energy of the completely helical peptide is also shown for reference. With an increase in λ, we see an increase in both the electrostatic energy and vdW energy. On comparing the vdW energy of the equilibrated system to completely helical peptide, we do not see an appreciable change in energy up to $\lambda < 0.66$ beyond which the vdW energy of the equilibrated structure increases due to the complete unfolding of the helix. However, we observe a decrease in the electrostatic energy of the equilibrated peptide compared to the completely helical peptide, which can be attributed either to the partial or complete unfolding of peptide minimizing the repulsion between the like charged groups of the peptide.
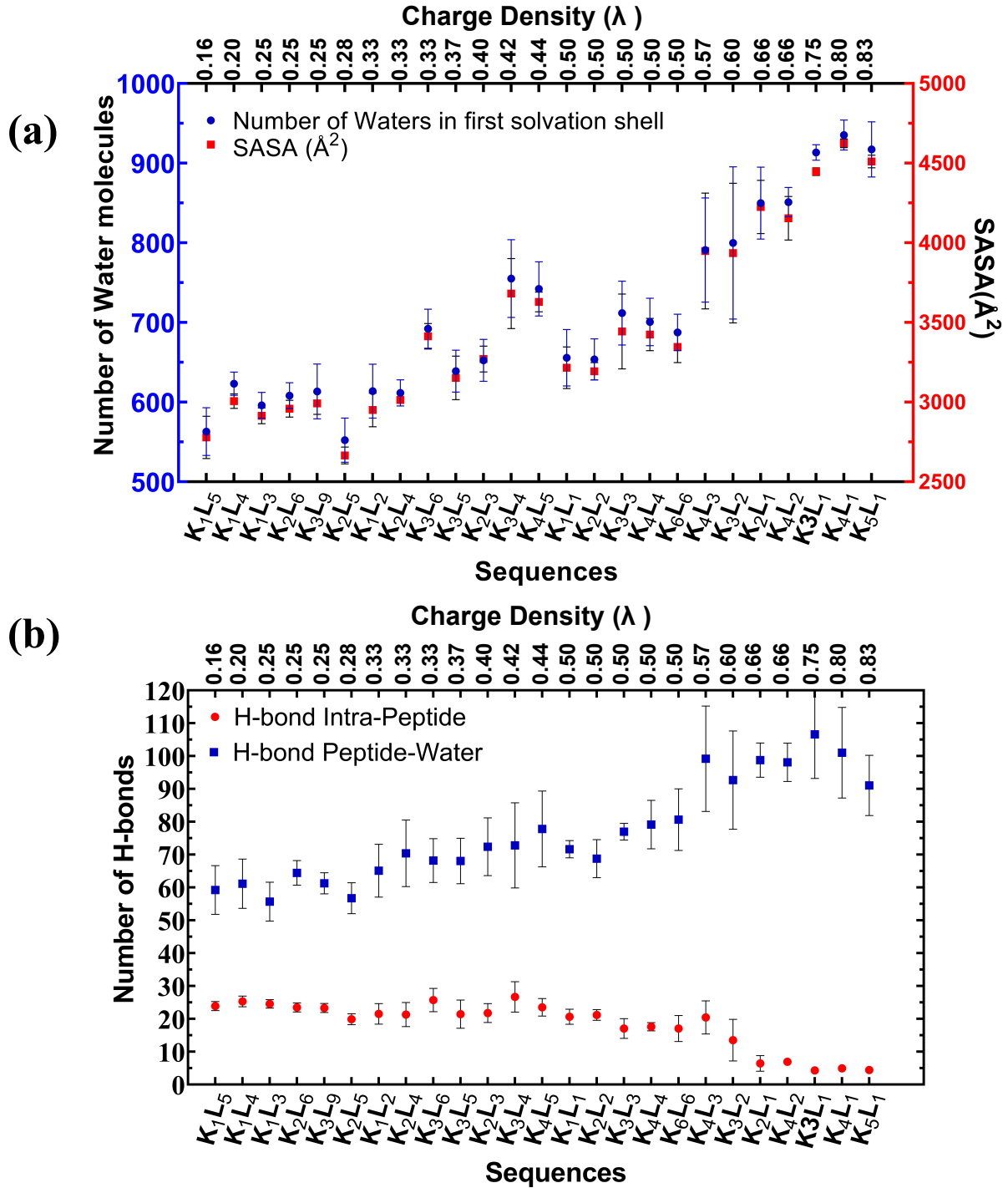
Figure 5: (a)Number of water molecules present in the first solvation shell of the protein at a distance within 6Å and SASA for different peptide sequences. The number of water molecules in the vicinity of peptides increased on increasing the charge density on the sequences (b) Number of intra-peptide hydrogen bonds and water-peptide hydrogen bonds for different peptide sequences. The number of intra-peptide hydrogen bonds decreased whereas the water-peptide hydrogen bonds increased causing the loss of helical content of the peptide

Figure 6: Energies for different sequences in NPT ensemble at 300K and 1atm. The electrostatic energy increased on increasing the charge content of the sequences whereas the vdW energy decreased because of the unfolding of the helix

Discussion

In this section, we would like to provide context to the above simulation findings vis a vis experiments. Our simulation findings on peptide sequences $(K_1L_2)_8$, $(K_2L_4)_4$, $(K_3L_6)_3$ with $\lambda = 0.33$ closely matches with the 22 residue sequence studied by Cornut et al[50] in terms of the charge density. The helical content calculated from the simulations and the secondary structure obtained through circular dichroism studies are in qualitative agreement. Further Cornut et.al also showed that by decreasing the length of the peptide at fixed charged density of $\lambda = 0.32$, there was a dramatic reduction in the helical content which is in line with the previous theoretical and computational studies.[51,52]

The current study emphasizes that the fraction of helical content is inversely proportional to the charge density. At the outset this results may appear not in agreement with previous experimental findings by Apte et.al[53] and De Grado *et.al*[54] who observed that peptides with similar charge density formed different secondary structures like $\alpha-$ helices or β-sheets depending on the patterning of Lysine and Leucine residues in the sequence. The results obtained by Apte et.al for sequences AcLKKLLKLLKKLLKL-OH and Ac-LKLKLKLKLKLKLKL-OH were upon adsorption of these peptides on a gold surface and not in bulk as in the present study. Further, in the work by De Grado et.al whose study predates Apte et.al, it is clearly stated that the secondary structure observed in the aqueous solution were strongly dependent on the peptide and salt concentration, and also on the length of the peptide. The induction of secondary structures on these peptides was only observed at high peptide concentration where protein-protein interactions stabilize the secondary structures. The current set of simulations was carried out at infinite dilution (presence of one peptide) and in the absence of salt concentration. Therefore it would not be possible to compare our current study with studies carried out at high salt and peptide concentrations.

Conclusion

In summary, we have performed extensive Molecular Dynamics simulations on homo-polypeptides and 25 co-polypeptide sequences of Lysine and Leucine to understand their helical stability. Charged homo-polypeptides completely lost their helical content due to the increased electrostatic repulsion between side chains of amino acid groups in the helical state. Co-polypeptides of Lysine and Leucine showed a gradual decrease in the helical content with an increase in the charge density up to $\lambda=0.6$, beyond which they completely transformed into coils. This unfolding of helices was also quantified by an increase in the radius of gyration of

the peptide, increased SASA and increased number of water molecules in the first solvation shell. At a fixed charge density, we did not observe a significant change in the helical content for different peptide sequences. Further, the peptide electrostatic energy decreased compared to a completely helical peptide indicating that the unfolding is driven by the electrostatic repulsion among the charged amino acid residues.

Conflicts of Interest

The authors declare no conflict of interest

Acknowledgement

Supporting Information Available

Figure S1: RDF between the Nitrogen atoms in the Lysine side chain for the helical conformation(initial conformation) and after unfolding(final conformation).

PDB IDs of all the proteins analyzed for the calculation of the charge density in the α-helices.

References

(1) Nelson, D. L.; Lehninger, A. L.; Cox, M. M. *Lehninger principles of biochemistry*; Macmillan, 2008.

(2) Yakimov, A.; Afanaseva, A.; Khodorkovskiy, M.; Petukhov, M. Design of stable α-helical peptides and thermostable proteins in biotechnology and biomedicine. *Acta Naturae ( )* **2016**, *8*, 70–81.

(3) Milletti, F. Cell-penetrating peptides: classes, origin, and current landscape. *Drug discovery today* **2012**, *17*, 850–860.

(4) Fischer, R.; Fotin-Mleczek, M.; Hufnagel, H.; Brock, R. Break on through to the Other Side—Biophysics and Cell Biology Shed Light on Cell-Penetrating Peptides. *ChemBioChem* **2005**, *6*, 2126–2142.

(5) Fujiwara, K.; Toda, H.; Ikeguchi, M. Dependence of α-helical and β-sheet amino acid propensities on the overall protein fold type. *BMC structural biology* **2012**, *12*, 1–15.

(6) Ihalainen, J. A.; Paoli, B.; Muff, S.; Backus, E. H.; Bredenbeck, J.; Woolley, G. A.; Caflisch, A.; Hamm, P. α-Helix folding in the presence of structural constraints. *Proceedings of the National Academy of Sciences* **2008**, *105*, 9588–9593.

(7) Paoli, M.; Liddington, R.; Tame, J.; Wilkinson, A.; Dodson, G. Crystal structure of T state haemoglobin with oxygen bound at all four haems. *Journal of molecular biology* **1996**, *256*, 775–792.

(8) Li, G.; Xia, X.; Long, Y.; Li, J.; Wu, J.; Zhu, Y., et al. Research progresses and applications of antimicrobial peptides. *Chinese Journal of Animal Nutrition* **2014**, *26*, 17–25.

(9) Mihajlovic, M.; Lazaridis, T. Charge distribution and imperfect amphipathicity af-

fect pore formation by antimicrobial peptides. *Biochimica et Biophysica Acta (BBA)-Biomembranes* **2012**, *1818*, 1274–1283.

(10) Huang, Y.-B.; He, L.-Y.; Jiang, H.-Y.; Chen, Y.-X. Role of helicity on the anticancer mechanism of action of cationic-helical peptides. *International Journal of Molecular Sciences* **2012**, *13*, 6849–6862.

(11) Dan, N.; Setua, S.; Kashyap, V. K.; Khan, S.; Jaggi, M.; Yallapu, M. M.; Chauhan, S. C. Antibody-drug conjugates for cancer therapy: chemistry to clinical implications. *Pharmaceuticals* **2018**, *11*, 32.

(12) Qiao, X.; Wang, Y.; Yu, H. Progress in the mechanisms of anticancer peptides. *Sheng wu Gong Cheng xue bao= Chinese Journal of Biotechnology* **2019**, *35*, 1391–1400.

(13) Stefureac, R.; Long, Y.-t.; Kraatz, H.-B.; Howard, P.; Lee, J. S. Transport of α-helical peptides through α-hemolysin and aerolysin pores. *Biochemistry* **2006**, *45*, 9172–9179.

(14) Fernández-Vidal, M.; Jayasinghe, S.; Ladokhin, A. S.; White, S. H. Folding amphipathic helices into membranes: amphiphilicity trumps hydrophobicity. *Journal of molecular biology* **2007**, *370*, 459–470.

(15) D. de Araujo, A.; Lim, J.; Wu, K.-C.; Xiang, Y.; Good, A. C.; Skerlj, R.; Fairlie, D. P. Bicyclic helical peptides as dual inhibitors selective for Bcl2A1 and Mcl-1 proteins. *Journal of medicinal chemistry* **2018**, *61*, 2962–2972.

(16) Eckert, D. M.; Kim, P. S. Design of potent inhibitors of HIV-1 entry from the gp41 N-peptide region. *Proceedings of the National Academy of Sciences* **2001**, *98*, 11187–11192.

(17) Finkelstein, A.; Badretdinov, A. Y.; Ptitsyn, O. Physical reasons for secondary structure stability: α-Helices in short peptides. *Proteins: Structure, Function, and Bioinformatics* **1991**, *10*, 287–299.

(18) Doig, A. J. Recent advances in helix–coil theory. *Biophysical chemistry* **2002**, *101*, 281–293.

(19) Rohl, C. A.; Baldwin, R. L. *Methods in enzymology*; Elsevier, 1998; Vol. 295; pp 1–26.

(20) Berger, A.; Linderstrøm-Lang, K. Deuterium exchange of poly-DL-alanine in aqueous solution. *Archives of biochemistry and biophysics* **1957**, *69*, 106–118.

(21) Ferretti, J. A.; Paolillo, L. Nuclear magnetic resonance investigation of the helix to random coil transformation in poly-α-amino acids. I. Poly-L-alanine. *Biopolymers: Original Research on Biomolecules* **1969**, *7*, 155–171.

(22) Daggett, V.; Levitt, M. Molecular dynamics simulations of helix denaturation. *Journal of molecular biology* **1992**, *223*, 1121–1138.

(23) Bixon, M.; Lifson, S. Solvent effects on the helix–coil transition in polypeptides. *Biopolymers: Original Research on Biomolecules* **1966**, *4*, 815–821.

(24) Dalgicdir, C.; Globisch, C.; Peter, C.; Sayar, M. Tipping the scale from disorder to alpha-helix: folding of amphiphilic peptides in the presence of macroscopic and molecular interfaces. *PLoS Computational Biology* **2015**, *11*, e1004328.

(25) Doty, P.; Wada, A.; Yang, J. T.; Blout, E. Polypeptides. VIII. Molecular configurations of poly-L-glutamic acid in water-dioxane solution. *Journal of Polymer Science* **1957**, *23*, 851–861.

(26) Nishigami, H.; Kang, J.; Terada, R.-i.; Kino, H.; Yamasaki, K.; Tateno, M. Is it possible for short peptide composed of positively-and negatively-charged "hydrophilic" amino acid residue-clusters to form metastable "hydrophobic" packing? *Physical Chemistry Chemical Physics* **2019**, *21*, 9683–9693.

(27) Marqusee, S.; Baldwin, R. L. Helix stabilization by Glu-... Lys+ salt bridges in short

peptides of de novo design. *Proceedings of the National Academy of Sciences* **1987**, *84*, 8898–8902.

(28) Meuzelaar, H.; Vreede, J.; Woutersen, S. Influence of Glu/Arg, Asp/Arg, and Glu/Lys salt bridges on α-helical stability and folding kinetics. *Biophysical journal* **2016**, *110*, 2328–2341.

(29) Maxfield, F. R.; Scheraga, H. A. The effect of neighboring charges on the helix forming ability of charged amino acids in proteins. *Macromolecules* **1975**, *8*, 491–493.

(30) Xie, M.; Liu, D.; Yang, Y. Anti-cancer peptides: Classification, mechanism of action, reconstruction and modification. *Open Biology* **2020**, *10*, 200004.

(31) J Boohaker, R.; W Lee, M.; Vishnubhotla, P.; LM Perez, J.; R Khaled, A. The use of therapeutic peptides to target and to kill cancer cells. *Current medicinal chemistry* **2012**, *19*, 3794–3804.

(32) Huang, Y.; Feng, Q.; Yan, Q.; Hao, X.; Chen, Y. Alpha-helical cationic anticancer peptides: a promising candidate for novel anticancer drugs. *Mini reviews in medicinal chemistry* **2015**, *15*, 73–81.

(33) Huang, C.-Y.; Klemke, J. W.; Getahun, Z.; DeGrado, W. F.; Gai, F. Temperature-dependent Helix- Coil transition of an alanine based peptide. *Journal of the American Chemical Society* **2001**, *123*, 9235–9238.

(34) Aftabuddin, M.; Kundu, S. Hydrophobic, hydrophilic, and charged amino acid networks within protein. *Biophysical journal* **2007**, *93*, 225–231.

(35) Moret, M.; Santana, M.; Zebende, G.; Pascutti, P. Self-similarity and protein compactness. *Physical Review E* **2009**, *80*, 041908.

(36) Jiang, Z.; Vasil, A. I.; Hale, J. D.; Hancock, R. E.; Vasil, M. L.; Hodges, R. S. Effects of net charge and the number of positively charged residues on the biological activity

of amphipathic α-helical cationic antimicrobial peptides. *Peptide Science* **2008**, *90*, 369–383.

(37) Chou, P. Y.; Scheraga, H. A. Calorimetric measurement of enthalpy change in the isothermal helix–coil transition of poly-L-lysine in aqueous solution. *Biopolymers: Original Research on Biomolecules* **1971**, *10*, 657–680.

(38) Epand, R. F.; Scheraga, H. A. The helix–coil transition of poly-L-lysine in methanol–water solvent mixtures. *Biopolymers: Original Research on Biomolecules* **1968**, *6*, 1383–1386.

(39) Nakazawa, T.; Ban, S.; Okuda, Y.; Masuya, M.; Mitsutake, A.; Okamoto, Y. A pH-dependent variation in α-helix structure of the S-peptide of ribonuclease A studied by Monte Carlo simulated annealing. *Biopolymers: Original Research on Biomolecules* **2002**, *63*, 273–279.

(40) Sacquin-Mora, S. Fold and flexibility: what can proteins' mechanical properties tell us about their folding nucleus? *Journal of The Royal Society Interface* **2015**, *12*, 20150876.

(41) Pettersen, E. F.; Goddard, T. D.; Huang, C. C.; Couch, G. S.; Greenblatt, D. M.; Meng, E. C.; Ferrin, T. E. UCSF Chimera—a visualization system for exploratory research and analysis. *Journal of computational chemistry* **2004**, *25*, 1605–1612.

(42) Humphrey, W.; Dalke, A.; Schulten, K. VMD: visual molecular dynamics. *Journal of molecular graphics* **1996**, *14*, 33–38.

(43) Huang, J.; MacKerell Jr, A. D. CHARMM36 all-atom additive protein force field: Validation based on comparison to NMR data. *Journal of computational chemistry* **2013**, *34*, 2135–2145.

(44) Phillips, J. C.; Hardy, D. J.; Maia, J. D.; Stone, J. E.; Ribeiro, J. V.; Bernardi, R. C.; Buch, R.; Fiorin, G.; Hénin, J.; Jiang, W., et al. Scalable molecular dynamics on CPU and GPU architectures with NAMD. *The Journal of chemical physics* **2020**, *153*, 044130.

(45) Feller, S. E.; Zhang, Y.; Pastor, R. W.; Brooks, B. R. Constant pressure molecular dynamics simulation: the Langevin piston method. *The Journal of chemical physics* **1995**, *103*, 4613–4621.

(46) Andersen, H. C. Rattle: A "velocity" version of the shake algorithm for molecular dynamics calculations. *Journal of computational Physics* **1983**, *52*, 24–34.

(47) Darden, T.; York, D.; Pedersen, L. Particle mesh Ewald: An N log (N) method for Ewald sums in large systems. *The Journal of chemical physics* **1993**, *98*, 10089–10092.

(48) Heinig, M.; Frishman, D. STRIDE: a web server for secondary structure assignment from known atomic coordinates of proteins. *Nucleic acids research* **2004**, *32*, W500–W502.

(49) Sung, S.-S. Folding simulations of alanine-based peptides with lysine residues. *Biophysical journal* **1995**, *68*, 826–834.

(50) Cornut, I.; Büttner, K.; Dasseux, J.-L.; Dufourcq, J. The amphipathic α-helix concept: application to the de novo design of ideally amphipathic Leu, Lys peptides with hemolytic activity higher than that of melittin. *FEBS letters* **1994**, *349*, 29–33.

(51) Ghosh, K.; Dill, K. A. Computing protein stabilities from their chain lengths. *Proceedings of the National Academy of Sciences* **2009**, *106*, 10649–10654.

(52) Zimm, B. H.; Bragg, J. Theory of the phase transition between helix and random coil in polypeptide chains. *The journal of chemical physics* **1959**, *31*, 526–535.

(53) Apte, J. S.; Gamble, L. J.; Castner, D. G.; Campbell, C. T. Kinetics of leucine-lysine peptide adsorption and desorption at-CH3 and-COOH terminated alkylthiolate mono-layers. *Biointerphases* **2010**, *5*, 97–104.

(54) DeGrado, W.; Lear, J. Induction of peptide conformation at apolar water interfaces. 1. A study with model peptides of defined hydrophobic periodicity. *Journal of the American Chemical Society* **1985**, *107*, 7684–7689.